Exploring the transport of plant metabolites using positron emitting radiotracers

Matthew R. Kiser,[1] Chantal D. Reid,[2] Alexander S. Crowell,[1] Richard P. Phillips,[2] and Calvin R. Howell[1]

[1]Physics Department, Duke University and Triangle Universities Nuclear Laboratory, Durham, North Carolina 27708.
[2]Biology Department and Nicholas School of the Environment and Earth Sciences, Duke University, Durham, North Carolina 27708.

(Received 31 December 2007; accepted 18 April 2008; published online 8 July 2008)

Short-lived positron-emitting radiotracer techniques provide time-dependent data that are critical for developing models of metabolite transport and resource distribution in plants and their microenvironments. Until recently these techniques were applied to measure radiotracer accumulation in coarse regions along transport pathways. The recent application of positron emission tomography (PET) techniques to plant research allows for detailed quantification of real-time metabolite dynamics on previously unexplored spatial scales. PET provides dynamic information with millimeter-scale resolution on labeled carbon, nitrogen, and water transport over a small plant-size field of view. Because details at the millimeter scale may not be required for all regions of interest, hybrid detection systems that combine high-resolution imaging with other radiotracer counting technologies offer the versatility needed to pursue wide-ranging plant physiological and ecological research. In this perspective we describe a recently developed hybrid detection system at Duke University that provides researchers with the flexibility required to carry out measurements of the dynamic responses of whole plants to environmental change using short-lived radiotracers. Following a brief historical development of radiotracer applications to plant research, the role of radiotracers is presented in the context of various applications at the leaf to the whole-plant level that integrates cellular and subcellular signals and/or controls. [DOI: 10.2976/1.2921207]

CORRESPONDENCE
Chantal D. Reid: chantal@duke.edu

Primary plant productivity sustains life on Earth and is a principal component of the planet's system that regulates atmospheric carbon dioxide (CO_2) concentration. A central goal of plant science is to understand the regulatory mechanisms of plant growth in a changing environment. Key to our understanding of productivity are the plant carbon and nutrient balances: how does the plant acquire and use resources for maintenance and protection to maximize individual growth and reproductive success? Aspects of this question have been examined independently at different organizational scales through genetic, molecular, organismal, and ecosystem studies. Increasingly, plant scientists are developing experimental techniques and quantitative models that enable them to integrate across scales for a more complete understanding of whole-plant responses to environmental change. For example, various genetic mutants are used to elucidate the role of specific metabolites in the control of photosynthesis (e.g., Swissa *et al.*, 1980; Sterky *et al.*, 1998); mutants are coupled with high-resolution imaging to elucidate the role of sugars in signaling and control of plant growth (e.g., Schurr *et al.*, 2006; Smith and Stitt, 2007), or of hormones in root gravitropic responses

(Chavarria-Krauser *et al.*, 2008); and chlorophyll fluorescence is measured remotely to estimate heterogeneous canopy photosynthesis in forests (Osmond *et al.*, 2004; Ananyev *et al.*, 2005). Although we do not fully understand several processes and feedback mechanisms important for plant growth, descriptive analytical models of plant photosynthesis that incorporate the complexity of growth regulatory networks will enable reliable quantitative predictions of plant responses to environmental change.

Through collaborative research within and among disciplines, scientists have developed new tools to address the integration of plant growth processes across spatial scales. These tools are helpful in developing a coherent description of plant development across scales of complexity from the genomic to the whole-plant physiological responses to the environment. At one end of the spectrum, this integration involves knowledge of biochemical regulatory networks that are controlled by gene expression (e.g., Tyson *et al.*, 2001; Tyson *et al.*, 2003). For example, using the unicellular yeast as our best-known physiological system, computer models of enzyme and protein-driven reaction networks are developed through sustained interaction between theory and experiment (e.g., Lapinskas *et al.*, 1995; Himmelbach *et al.*, 1998; Buchwald and Sveiczer, 2006). At the leaf level in plants, the simple biochemical model of photosythesis developed by Farquhar and colleagues (Farquhar *et al.*, 1980) has been extended to describe a network of enzyme-driven biochemical reactions (Zhu *et al.*, 2007). Collaborations between theoretical biologists and experimentalists are enabling the development of increasingly more sophisticated and complete computer models of biochemical regulatory reaction networks in systems biology. At the other end of the spectrum, canopy photoysnthesis models couple processes at the individual leaf level with canopy and remote sensing data to integrate productivity at regional and global scales (e.g., Field *et al.*, 1995; Chen and Coughenour, 2004; Sasai *et al.*, 2007). These large scale models integrate the plant response to environmental stresses. Intermediate to these extremes, regulatory processes at the whole-plant level sense and respond to external limiting factors that control productivity. The use of short-lived radioistopes in whole-plant studies can help elucidate the processes that link the enzyme-driven biochemical reactions to the physiological responses of plants to environmental stimuli (Fig. 1).

Plant growth and environmental change

Plant productivity is strongly influenced by environmental stresses that include drought, temperature extremes, nutrient

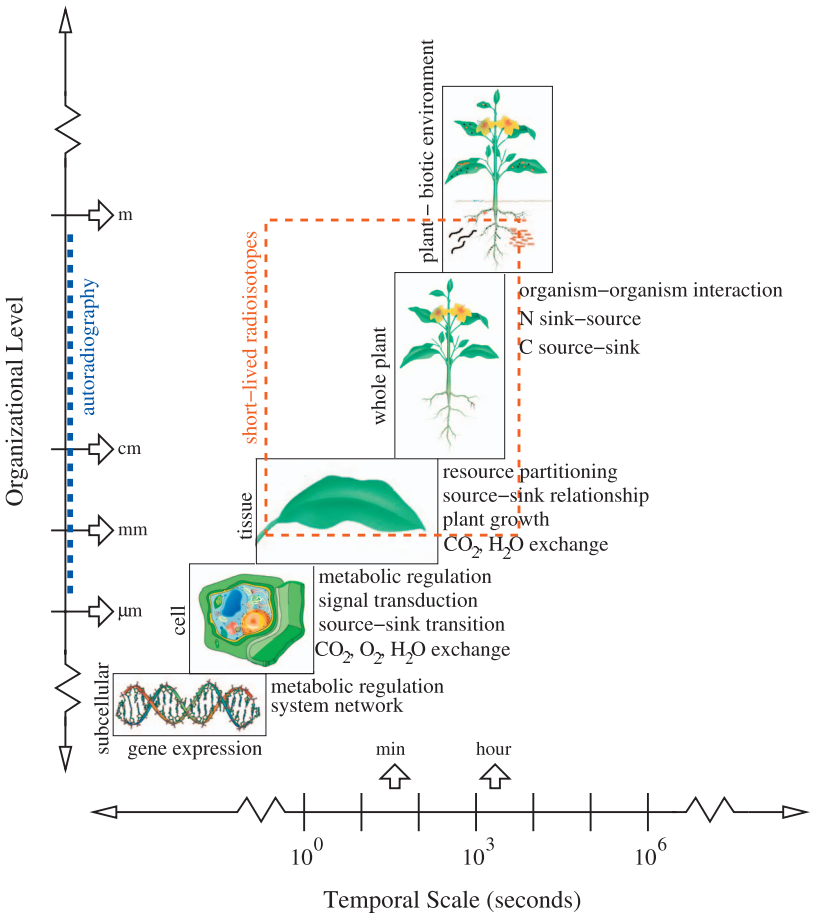

Figure 1. Hierarchical temporal and spatial processes of plant growth and development (based on Osmond, 1989). Different processes at the subcellular and cellular level can link to higher organizational levels via signal transduction. At small spatial scales autoradiography, which requires disturbance of the plant system, provides detailed images of radiotracer accumulation. At the tissue, whole-plant, and plant microenvironment levels, dynamic processes can be measured using short-lived positron-emitting radioisotopes with gamma-ray detection and imaging techniques.

limitation, and predator or pathogen pressure. All are likely to increase with global climate change, and the impact will vary regionally (e.g., Fischlin *et al.*, 2007). Although we have a good understanding of the photosynthetic process itself, detailed understanding is still missing for how plants sense chronic stresses (e.g., drought, low nutrient availability) and heterogeneous changes in the environment (e.g., sunflecks) that can result in short-term stresses, and the consequent impact of such stresses on growth and development. Osmond (1989) once forecasted that the now commonly used chlorophyll fluorescence technique could be a useful tool to scale our understanding of stress on photosynthesis from small-scale (within leaf tissue) indicator to large-scale (forest canopy) integrator (Jones and Morison, 2007). Similarly, we predict that short-lived radioisotope techniques will provide data that are crucial for developing models that quantitatively link the underlying biochemical reactions to physiological responses, i.e., to model the complexity of plant growth and development across different scales (Fig. 1). For example, sugars, which are produced in source leaves and needed in developing sinks, are both sensing and signaling molecules between cells and between organs (e.g., review by Rolland *et al.*, 2006). Sugar signaling can interact with other signals (e.g., hormones) to control plant development under different environmental conditions. As sensors or integrators of stress, sugars and other signal molecules rely on the phloem for long-distance transport (Lough and Lucas, 2006). Coupling the dynamic transport of the signal in response to environmental stress with gene expression in transgenic plants can provide us with better predictive models to understand integrated plant development and growth. A better mechanistic understanding of the phloem transport itself is in progress (Minchin and Lacointe, 2005; Thompson, 2006) and will benefit from dynamic measurement techniques. At a larger spatial scale, chemical signals are also used for communication between plants (competition or facilitation), or between plant and pathogen or microbes (Paiva, 2000). The availability of new techniques or novel applications of established methods can help decipher the role of metabolite transport and regulation.

Imaging technology and plant science

A variety of technologies are available that enable researchers to span a wide range of spatial scales in plant studies, from submicron resolution using optical microscopy techniques and fluorescent markers (Stephens and Allan, 2003; Haustein and Schwille, 2007) to millimeter-scale resolution using x-ray computed tomography (e.g., Kaestner *et al.*, 2006) and magnetic resonance imaging (MRI; e.g., MacFall *et al.*, 1990; Windt *et al.*, 2006). Dynamic processes can be imaged using time-lapse fluorescence microscopy with micron-scale resolution by taking successive images at the microsecond to millisecond time range (Weijer, 2003; Rieder and Khodjakov, 2003). For example, this technique has been used to determine patterns of the dominant gene expression in developing roots of *Arabidopsis* (Brady *et al.*, 2007). At a larger spatial scale (tenths of mm), MRI has been employed in medicine to visualize anatomical structure, as well as in plants to observe water content in and around root systems (e.g., MacFall *et al.*, 1990). In addition, techniques that use short-lived radioisotopes with gamma-ray detection provide the capacity to visualize dynamic transport and allocation of metabolites at large distance scales and consequently give information important for understanding whole-plant physiological responses to environmental change in real time. The combined application of these techniques provides detailed information about biological structure and function over spatial dimensions ranging from cells to entire organisms and between-organism interactions.

Coordination between the sensing and signal transport through the plant and/or out of the plant into the environment requires dynamic measurement methods. Short-lived radioisotopes are already used successfully at high specific activity to show the transport of jasmonate, a signal metabolite involved in plant defense, in whole plants (Thorpe *et al.*, 2007). Additionally, Ferrieri and colleagues assessed the role of recently fixed carbon with short-lived radiotracers and demonstrated that treatment of poplar seedlings with jasmonic acid increases isoprene emission (Ferrieri *et al.*, 2005), leaf export of mobile sugar (Babst *et al.*, 2005), and plant metabolism of carbon tetrachloride (Ferrieri *et al.*, 2006). Carbon-11 tracer measurements designed to study carbon metabolism dynamics cover a wide range of spatial scales within plants. For example, Minchin and colleagues have measured unloading and reloading of photoassimilate in bean stem (Minchin and Thorpe, 1987); carbon partitioning to whole versus surgically modified pea ovules (Minchin and Thorpe, 1989); changes in partitioning to soybean root nodules following treatment of the root system with nitrate (Thorpe *et al.*, 1998); the short and long-term effects of photosynthate availability on carbon partitioning to apple fruits (Minchin *et al.*, 1997); the effect of electric shock and cold shock on phloem transport (Pickard *et al.*, 1993); and the effects of temperature (Minchin *et al.*, 1994) and osmotica (Williams *et al.* 1991) on carbon partitioning in split root systems of barley. Additionally, ^{11}C radiotracer techniques were applied in an ecological context to measure plant response to herbivory by nematodes (Freckman *et al.*, 1991) and grasshoppers (Dyer *et al.*, 1991) at Duke University, and more recently, by inducible response to simulated leaf herbivory (Babst *et al.*, 2005; Schwachtje *et al.*, 2006). Likewise, measurements using short-lived isotopes are valuable in studies of root growth dynamics and nutrient uptake in a heterogenous environment.

Positron emission tomography (PET) is a noninvasive imaging technique that can achieve spatial resolution on the order of millimeters and provide quantitative information

about dynamic physiological processes over a relatively large field of view. PET utilizes radioactive nuclei to label biologically active molecules. These systems have been used clinically for the diagnosis of human disease for about 30 years (Ter-Pergossian *et al.*, 1975; Rohren *et al.*, 2004), and many research centers now employ microPET instruments to better understand disease by studying small animals (Cherry *et al.*, 1997; Chatziioannou, 2002). In addition to biomedical applications, PET techniques are used to study the regulation of plant growth and development via metabolite transport. Because plants are sessile organisms, they have developed adaptations to deal with a heterogeneous environment, which often includes metabolite signaling to induce a cascade of physiological responses. Plant labeling entails the integration of short-lived positron-emitting isotopes such as carbon-11 (^{11}C), nitrogen-13 (^{13}N), oxygen-15 (^{15}O), and fluorine-18 (^{18}F) into biologically active molecules, nutrients, or compounds. The radiotracers (i.e., labeled molecules) are absorbed via normal metabolism and distributed throughout the plant. *In vivo* detection of the gamma rays emitted by the radioisotopes enables researchers to track the transport and distribution of the radiotracers in the plant as a function of time. The short radioactive half-lives of the radiotracers and the noninvasive detection of the decay products allow the same plant to be tested multiple times without destructive sampling to determine its response to environmental changes. Additionally, a suite of different short-lived radiotracers can be applied to the same plant in a short period of time to investigate the transport and allocation of various metabolites (Caldwell *et al.*, 1984;Grodzinski *et al.*, 1984). These features make short-lived positron-emitting radiotracers attractive candidates for studying the dynamics of metabolite transport in plants. Also, the time-ordered data obtained with radiotracers provides the information required to causally connect plant responses to specific environmental changes.

While earlier studies monitored radiotracer transport and accumulation on a coarse spatial scale, recent experiments use PET techniques to produce high-resolution images of radiotracer transport and allocation (e.g., Keutgen *et al.*, 2005). In this perspective we describe recent studies using short-lived radioisotopes to examine aspects of plant growth at different spatiotemporal scales. We start with a brief review of the historical development of radiotracer techniques followed by a discussion of the general use of positron emission techniques in plant research. We concentrate on a radiotracer labeling system that is based on a hybrid gamma-ray detection platform being developed at Duke University for positron emission imaging and counting in plant studies. This radiotracer system is primarily for studies of carbon, nutrient, and water transport and allocation in plants.

HISTORICAL DEVELOPMENT OF THE APPLICATION OF RADIOTRACERS TO PLANT STUDIES

A variety of techniques are used to measure the transport and distribution of substances in plants. These include methods that employ both stable and radioactive isotopes. Examples include real-time tracing of short-lived radioisotopes (e.g., ^{11}C, ^{13}N), measuring accumulation of long-lived radioisotopes (e.g., ^{14}C) and stable isotopes (e.g., ^{13}C, ^{15}N), and studying water flow with MRI.

The use of short-lived positron emitters

The first plant studies using short-lived radioisotopes were performed nearly 70 years ago by Ruben *et al.* (1939) in their work on photosynthesis using ^{11}C. Because of the short life of ^{11}C (20.4 min), Ruben soon searched for and discovered a long-lived radioisotope, ^{14}C (half-life 5730 years) that has been used extensively in metabolite accumulation (Gest, 2005; and see below). Nevertheless, since then many types of plant physiology studies have been performed using carbon-11 dioxide ($^{11}CO_2$) as a radiotracer. Labeled $^{11}CO_2$ is particularly useful in studies of carbohydrate source-sink relationships in plants. Because CO_2 is the primary substrate for photosynthesis, $^{11}CO_2$ is incorporated into plant tissue as photoassimilates, i.e. carbohydrates that can be tracked through the plant by detecting the gamma radiation emitted in the decay of ^{11}C nuclei. The isotopic discrimination between $^{11}CO_2$ and $^{12}CO_2$ during photosynthesis is likely similar in magnitude to that between ^{13}C and ^{12}C, which is on the order of a few percent (Farquhar *et al.*, 1982; Thorpe and Minchin, 1991). The ^{11}C nucleus decays by emitting a positron (i.e., an anti-electron) and has a radioactive half-life of 20.4 min. Positrons emitted by the decay of ^{11}C nuclei lose energy by collisions in matter until they reach thermal energies and annihilate with an electron. This annihilation produces two gamma rays (high energy photons, each with 511 keV energy) that are emitted collinearly and in opposite directions to conserve linear momentum. These gamma rays are attenuated very little by the tissue of small plants and may be detected singly with collimated detectors or in coincidence to trace the distribution of ^{11}C in real time and *in vivo* (Minchin and Thorpe, 2003).This technique allows for multiple radiotracer labelings of the same plant, which leads to a better understanding of biological variations within a single organism. Because the radioactive half-life of ^{11}C is about 20 min, it is particularly useful for the study of short-term effects of environmental stimuli on carbon translocation dynamics and source-sink relationships. The fundamental limit on the spatial resolution achievable using positron-emitting tracers is governed by the finite range that the positrons travel inside the material before losing all their kinetic energy via ionization and annihilating with an electron. This travel range is a function of the initial kinetic energy of the positron and therefore is different for each radiotracer isotope (Table I). However, it is generally the main

Table I. Properties of positron-emitting isotopes used to measure metabolite transport and allocation in plants. E_{max} and E_{mean} are the maximum and mean energy of the emitted positron, and $t_{1/2}$ is the radioactive half-life of the isotope. The maximum and mean range of the positrons is given for water because this is a close approximation to plant tissue. The data in this table are from Bailey *et al.* (2003).

Radioisotope	E_{max} (MeV)	E_{mean} (MeV)	$t_{1/2}$ (min)	Max range in water (mm)	Mean range in water (mm)
^{11}C	0.959	0.326	20.4	4.1	1.1
^{13}N	1.197	0.432	9.96	5.2	1.5
^{18}F	0.633	0.202	109.8	2.4	0.6
^{15}O	1.738	0.696	2.03	7.3	2.5

source of uncertainty that limits the accuracy of determining the positron production location (i.e., spatial resolution) to a few millimeters.

For improved spatial resolution, positron-emitting radiotracers can also be imaged using positron autoradiography, which gives spatial detail on the order of hundreds of microns (Schmidt and Smith, 2005) by direct detection of the positrons. This resolution is about an order of magnitude better than that achievable with PET because the positron energy is deposited directly on the phosphor imaging plate before it has the opportunity to annihilate. Direct detection of the positron eliminates the uncertainty in radiotracer location that is due to the distance the positron travels before annihilating. This technique has been applied in whole-plant studies to determine metabolite partitioning at the end of a labeling period using phosphor plate imaging of the plant (Babst *et al.*, 2005; Ferrieri *et al.*, 2006). Positron autoradiography has also been used to investigate radiotracer allocation in detached leaves of tobacco plant (Thorpe *et al.*, 2007). While positron autoradiography provides much better spatial detail than PET, real-time dynamic information cannot be attained without disturbing the labeled organism. Tanoi *et al.* (2005) have demonstrated an imaging system in which the labeled plant is placed directly against a vertically mounted imaging plate. Sequential images provide information about flow dynamics, but exposures must be performed in the dark because fluorescent light can erase the information stored in the imaging plate. A system of this type could be used to image plant roots without disrupting the biological system, but it is not ideal for above-ground regions of the plant that behave differently in light and dark conditions. PET cannot provide the same level of spatial detail, but it requires minimal disturbance to the organism.

In addition to ^{11}C, other short-lived positron-emitting isotopes have been used for plant physiology studies. Nitrogen-13 (^{13}N) decays by positron emission with a radioactive half life of 9.96 min. This isotope can be introduced to plants in the form of ^{13}N-labeled nitrate (e.g., Glass *et al.*, 1985) or ammonium (e.g., Kronzucker *et al.*, 1995c) ions in solution, or as ^{13}N-labeled nitrogen gas (e.g., Bishop *et al.*, 1986). The ^{13}N-labeled substances are generally applied to plant roots to study nutrient absorption and transport in the plant under various environmental conditions (e.g., McNaughton and Presland, 1983). To extract root nitrate flux characteristics, compartmental models have been applied to ^{13}N data from barley (Lee and Clarkson, 1986; Siddiqi *et al.*, 1991; Ritchie, 2006), maize seedlings (Presland and McNaughton, 1984), and spruce seedlings (Kronzucker *et al.*, 1995a, 1995b). Additionally, the tracer efflux kinetics of ^{13}N-labeled ammonium have been examined using compartmental analysis in the roots of barley (Britto and Kronzucker, 2003), maize seedlings (Presland and McNaughton, 1986), spruce seedlings (Kronzucker *et al.*, 1995c, 1995d), and rice (Wang *et al.*, 1993a; Kronzucker *et al.*, 1998), as well as in leaf segments of wheat (Britto *et al.*, 2002). Kinetic models that parameterize nutrient uptake have also been developed based on ^{13}N-labeled nitrate influx measurements in barley roots (Lee and Drew, 1986) and ^{13}N-labeled ammonium influx in rice roots (Wang *et al.*, 1993b). Each of these experiments combined the use of ^{13}N-labeled radiotracers with rigorous mathematical treatment to extract meaningful information about nitrogen flow in a particular region of an intact plant.

Oxygen-15 (^{15}O) is another short-lived radioisotope that decays by positron emission; its radioactive half-life is 2.03 min. Generally, a water source ($H_2{}^{15}O$) is produced and introduced to the plant through the root bathing solution. Gamma-ray detectors (or a positron emission imaging system) are then used to monitor radiotracer accumulation in sections of the plant to observe water transport (Kiyomiya *et al.*, 2001a; Nakanishi *et al.*, 2003, Tanoi *et al.*, 2005). Due to its very short half-life, ^{15}O is only useful for tracing phenomena occurring on a short time scale. However, the longer-lived isotope fluorine-18 (^{18}F; 109.8 min radioactive half life) has been used as a proxy for tracing the dynamics of water transport because fluorine ions bind readily to water molecules (Kume *et al.*, 1997; Nakanishi *et al.*, 2001c). The prolonged half-life of ^{18}F makes it a more attractive candidate for measuring longer-term phenomena, although ^{18}F labeling likely tracks the movement of fluorine ions more so than water molecules (Nakanishi *et al.*, 2001b). In addition, MRI offers an alternative for measuring the long-term dynamics of water transport in plants (Windt *et al.*, 2006; Van As, 2007).

The dynamic information obtained from radiotracer experiments is used to investigate time-dependent changes within the labeled plant. Short-lived radiotracer experiments with $^{11}CO_2$ use either pulse-labeling, where $^{11}CO_2$ gas is supplied to a portion of the plant in a short burst (pulse), or continuous labeling, where the ^{11}C activity in the labeling system is kept fairly constant by supplying $^{11}CO_2$ at regular intervals (Thorpe and Minchin, 1991) or by a continuous production system (Magnuson *et al.*, 1982). The continuous labeling technique is particularly useful for studying diurnal patterns and other time-dependent plant responses, such as those due to environmental changes (e.g., shading; Thorpe and Minchin, 1991). Pulse-labeling can also be used to measure metabolite dynamics in plants. For example, time-dependent analysis techniques are applied to radiotracer data obtained from pulse-labeling experiments to determine the plant response during the labeling period (e.g., Minchin and Grusak, 1988). Alternatively, the environmental conditions of the plant can be modified between pulse-labeling periods or similar plants grown in different environmental conditions can be pulse-labeled to measure plant responses.

Long-time scale measurements with isotopic analysis techniques

The use of short-lived positron emitters provides the ability to perform real-time substance accumulation and flow measurements *in vivo*. However, a few important constraints should be considered when designing experiments that use short-lived radioisotopes. First, the short radioactive half-life requires that experiments be performed near the isotope production facility. Second, its short radioactive half-life limits the dynamic phenomena that can be observed to those with characteristic time constants on the order of a few hours. Last, high initial radioactivity is needed to observe the radiotracer transport and allocation over long periods of time (e.g., nine half lives for ^{11}C), so sufficient radiation shielding must surround the labeling region.

For measuring carbon dynamic processes of a longer time scale than achievable with short-lived radioisotopes, measurement techniques based on the stable ^{13}C isotope or the long-lived ^{14}C radioisotope can be used. However, determination of ^{13}C accumulation in plant tissue requires destructive harvesting of the labeled plant for mass spectrometry. There are also two major drawbacks with ^{14}C labeling: (1) due to the long half-life, a single plant cannot be labeled multiple times, and (2) the low energy beta particle emitted from ^{14}C decay has a small probability of escaping plant tissue thereby drastically reducing the number of cases where *in vivo* counting techniques can be used. For example, detection of the ^{14}C beta particles in plant leaves has been used in autoradiography studies of phloem loading, unloading, and transport (Fritz *et al.*, 1983; Turgeon, 1987; Turgeon and Wimmers, 1988). While beta particles emitted in ^{14}C decay may escape a thin leaf, they will likely be absorbed by thicker shoot or root tissue. Thus, the labeled plant must be destructively harvested at the end of a labeling period, and ^{14}C accumulation is quantified by either detecting the beta particles emitted from various plant tissues or by accelerator mass spectrometry (Reglinski *et al.*, 2001). The ^{14}C-radio-labeled plant tissue has also been sampled destructively for studies of carbon allocation of particular metabolites (e.g., phenolics; Margolis *et al.*, 1991). These methods provide information about carbon allocation but give no insight into carbon transport dynamics in the same plant.

Development of data analysis techniques

Over the last 30 years, the considerable advancements made in gamma-ray detection, imaging, and analysis techniques have enabled high precision quantitative studies of plants using short-lived radioisotopes. The pioneering work of Peter Minchin and colleagues (e.g., Minchin and McNaughton, 1984; Minchin and Thorpe, 1987, 1989) established the foundation for this field using collimated single detectors. One of Minchin's most important contributions was the development of analysis techniques that provide the framework for quantitative interpretation of tracer profiles. Tracer profiles are measurements of the spatial distributions of radiotracer inside the plant as a function of time. Using a statistical analysis derived from transfer functions in physics, Minchin developed an input-output model to determine properties of the transport system tracer profile data (Minchin, 1978). The transfer function describes the change in shape of the tracer profile between the system input and output and provides an alternate description of the system that can be used to calculate the output response for any given input (Cadzow, 1973, Ch.7). This type of analysis makes no assumptions about the physical mechanisms involved but allows physiologically relevant parameters to be calculated (Minchin and Troughton, 1980). Transfer function analysis has been applied to many sets of ^{11}C tracer profile data to extract physically meaningful information about carbon allocation and transport in plants. Because input-output models provide a mathematical description of the data and physically relevant parameters, any mechanistic model should be consistent with the statistical modeling results.

In addition to transfer function analysis, mechanistic models have been used to describe radiotracer transport and allocation. Minchin *et al.* (1993) applied a transport-resistance (TR) model proposed by Thornley (1972; reviewed by Minchin and Lacointe, 2005) to explain source-sink dynamics using ^{11}C radiotracer data. The TR model is based on Münch's original hypothesis that photoassimilate flow is driven by an osmotically generated pressure gradient. Bancal and Soltani (2002) extended this model to consider the source term as an activity of solute production rather than a compartment concentration and to include changes in sap viscosity. The TR model does not incorporate all the intrica-

cies of the transport system, but it does provide sufficient mechanistic detail to describe the phenomena observed in whole-plant experiments. In fact, Thornley (1998) suggests that a TR model needs to be the starting point for all more complex models, as this incorporates the only two significant processes, transport and chemical conversion, that result in allocation.

Mechanistic models of phloem transport can be used to fit tracer profile data and estimate physical parameters (e.g., Moorby *et al.*, 1963), but these models may assign unnecessary complexity to the system. Compartmental analysis (e.g. Fares *et al.*, 1988) considers the flow of carbon through a series of partitions of characteristic kinetics, so it does not assume any explicit mechanism for phloem transport. However, compartmental analysis does provide physiological parameters that can be directly compared to those predicted by mechanistic models (e.g., Moorby and Jarman, 1975). Detailed mathematical models of phloem transport have been proposed (e.g., Goeschl *et al.*, 1976; Daudet *et al.*, 2002; Thompson, 2006); these have not been directly compared to radiotracer data, but their predictions can be compared to the physiologically relevant parameters obtained using nonmechanistic analysis methods.

^{11}C LABELING AT DUKE UNIVERSITY

The first plant studies using short-lived radioisotopes at Duke University were performed in the 1980's. These took advantage of the close proximity of the Duke University Plant Growth Facilities (Phytotron) and the Triangle Universities Nuclear Laboratory (TUNL). The ^{11}C was produced using the TUNL 4 MeV Van de Graaff accelerator. A beam of ^{3}He nuclei was directed on a $^{12}CO_2$ flowing gas target to produce $^{11}CO_2$ continuously via the $^{12}C+{}^{3}He \rightarrow {}^{11}C+{}^{4}He$(Q=+1.86 MeV) reaction (Magnuson *et al.*, 1982). Later, $^{11}CO_2$ was also produced at the Duke University Medical School Cyclotron and transferred to the Phytotron using a shielded transporter (McKinney *et al.*, 1989) for pulse-labeling experiments. With improved technology a new initiative is under way to study plants using short-lived radiotracers at Duke University. The initial focus of the research program is to measure physiological responses of plants to environmental changes and to measure the rates of physiological processes that are important for plant growth. In this research, ^{11}C is produced with the TUNL FN tandem Van de Graaff accelerator by bombarding a nitrogen (N_2) gas-filled target cell with an energetic (~10 MeV) beam of protons for about 30 min. This radioactive-substance production method is based on the $^{14}N+p \rightarrow {}^{11}C+{}^{4}He$(Q=−2.92 MeV) reaction that was used by Jahnke *et al.* (1981). We prefer this reaction over the $^{10}B+d \rightarrow {}^{11}C+n$(Q=+6.46 MeV) reaction, which is commonly used with low-energy electrostatic accelerators, because it can be implemented more easily and with a higher efficiency for producing ^{11}C tagged carbon dioxide. For example, we produce 25 milliCuries of $^{11}CO_2$ in 30 min with 1.5 μA of proton beam on a nitrogen gas target compared to 10 milliCuries produced by Minchin and colleagues (More and Troughton, 1973) by bombarding a ^{10}B target with 30 μA of deuterons for the same length of time.

A schematic diagram of the recently developed $^{11}CO_2$ radiotracer gas system at Duke University is shown in Fig. 2. The $^{11}CO_2$ gas is produced in the tandem accelerator laboratory at TUNL, and the plant labeling measurements are performed at the Duke Phytotron in a specially modified environmental growth chamber. The present system provides researchers with pulse-loading capability and was designed to make upgrading for continuous loading measurements straightforward. The $^{11}CO_2$ gas is produced by bombarding a target cell pressurized to 7.8 atmospheres with research-grade N_2 gas with a proton beam. The contents of the produc-

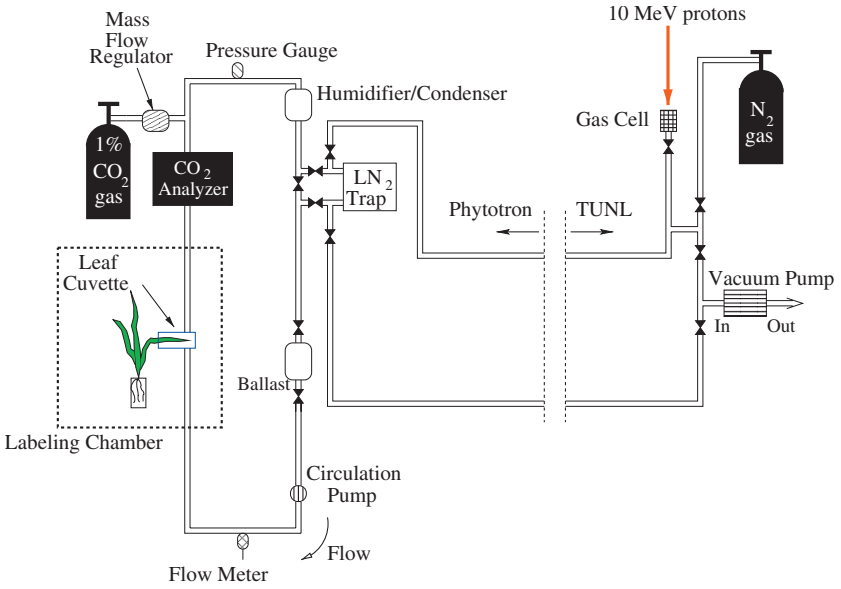

Figure 2. $^{11}CO_2$ production, transport and, labeling system at Duke University. The $^{11}CO_2$ gas is produced in the tandem accelerator at TUNL ($p+{}^{14}N \rightarrow {}^{11}C+{}^{4}He$) and transferred to the Duke University Phytotron via tubing in underground conduits. $^{11}CO_2$ gas from the target cell is collected in a lead-shielded liquid nitrogen cooled trap at the Phytotron. Other gases (mostly nitrogen and carbon monoxide) from the target cell are pumped back through the exhaust system at TUNL. The present system has pulse-loading capability only. A pulse of $^{11}CO_2$ gas is introduced into the labeling loop by warming the CO_2 trap to room temperature and opening the valves that isolate the trap from the loop so that the air in the loop flows through the trap, thereby mixing with the radioactive $^{11}CO_2$ gas.

tion cell, which is N_2 gas with a minute mixture of radioactive tagged gases, is transferred through tubing in an underground conduit approximately 100 m to the labeling system in the Phytotron. In a typical isotope production run the proton beam is kept on the target gas cell for about 30 min. The main radioactive gases produced in the process are ^{11}CO, $^{11}CO_2$, and ^{14}O tagged O_2. The ^{14}O is produced by the $^{14}N+p \rightarrow {}^{14}O+n$ reaction ($Q=-5.93$ MeV). It decays by positron emission with a radioactive half life of 1.2 min compared to the 20.3 min half life of ^{11}C. After a production run the radioactive gas mixture in the target cell is slowly pumped through a liquid-nitrogen cooled trap where the CO_2 is frozen, the O_2 is liquefied and the N_2 and CO gases are vented into a high-flow gas exhaust system in the tandem accelerator laboratory. Though not shown in Fig. 2, the LN-cooled trap is inside a 4-in.-thick lead shielding enclosure. Most of the ^{14}O that is trapped along with the CO_2 decays before the gas is loaded into the labeling loop. The nominal activity of trapped $^{11}CO_2$ at the beginning of each labeling period is about 30 milliCuries ($\sim 10^9$ decays per second). After warming the trap to room temperature, the $^{11}CO_2$ gas is injected as a pulse into the labeling loop. The loop contains diagnostic instrumentation and control components, as well as a temperature-controlled leaf cuvette (Fig. 2). The $^{11}CO_2$ is mixed with air in the closed loop and introduced to the plant by flowing the air over a leaf that is in a sealed cuvette. The concentration of the labeled $^{11}CO_2$ is negligible compared to the controlled atmospheric [$^{12}CO_2$]; at the beginning of a labeling measurement the ratio of $^{11}CO_2$ to $^{12}CO_2$ molecules is about $1:10^9$. The $^{11}CO_2$ is metabolized via photosynthesis into ^{11}C-labeled photoassimilates that are tracked through the plant. The radiotracer experiments take place inside a controlled-environment growth chamber at the Phytotron that allows for maintenance of abiotic factors such as temperature (12°–35° C when fully lit and 2°–30° C when dark), light intensity (up to 350 μmol m^{-2} s^{-1} photosynthetically active radiation), and atmospheric CO_2 concentration (200–1000 μmol mol^{-1}). The chamber can replicate growth conditions of the plant in its natural environment and/or its experimental growth conditions, or it can be adjusted to a novel environment for short-term acclimation experiments.

Development of low spatial resolution 2D PET imaging

To gain experience with PET measurement techniques for plant applications and to develop image reconstruction software and quantitative data analysis tools, a prototype two-dimensional (2D) planar PET imager was constructed using existing hardware at TUNL. This prototype imager is composed of two planar arrays of cylindrical cesium fluoride detectors (25 mm diameter × 45 mm thick), with each array containing 10 detectors (Fig. 3). This arrangement provides a spatial resolution of about 1 cm in both the horizontal and vertical directions over a field of view (FOV) of approximately 12 cm (width) × 20 cm (height). The dimensions of the imager and the detector positions within each array were chosen to cover a specific FOV while also providing smooth geometric detection efficiency across the image plane. The image plane is located midway between the parallel planes defined by the front surfaces of the detector arrays. Coincidence detection of the back-to-back gamma rays emitted from electron-positron annihilation is used to initiate the recording of information associated with the decay of ^{11}C nuclei inside the plant tissue. The density distribution of the electron-positron annihilation sites is reconstructed on the image plane using the detector hit pattern data that are stored for each coincidence event. The source of the gamma rays for each event is projected onto the image plane at the point where the line connecting the centers of the two detectors involved in the coincidence intersects the image plane. The count for each event is distributed over several pixels in the image plane using a spatial probability distribution function that accounts for the finite size and the geometric arrangement of the detectors. Each event is recorded with a time stamp thereby providing the capability of tracing substance flow between any regions within the imager FOV. The information available from the images is limited spatially by the resolution of the imager and temporally by the period of time needed to accumulate adequate counting statistics in the regions of interest.

Trade-offs between spatial resolution and the area of the FOV are often necessary to make the final cost of the imager fit budget constraints. For example, the positron-emitting tracer imaging system (PETIS) developed at the Japan Atomic Research Institute was first used to measure uptake and transfer of ^{18}F in soybean with 2.5 mm spatial resolution in a 6 cm × 5 cm FOV (Kume *et al.*, 1997). While this spatial resolution is four times finer than that of the Duke prototype PET device, the imaging area is reduced by about a factor of 8. Since this original application, the PETIS device has been used to visualize translocation of ^{11}C-labeled methionine in barley (Nakanishi *et al.*, 1999), ^{13}N-labeled nitrates in soybean plants (Ohtake *et al.*, 2001), ^{13}N-labeled ammonium in rice (Kiyomiya *et al.*, 2001b), and ^{15}O-labeled water in soybean plants (Nakanishi *et al.*, 2001a). The primary limitation of the original PETIS was the small FOV. By adding two pairs of detector modules with dimensions similar to the original instrument, the PETIS detection area was increased to approximately 5 cm × 15 cm (Keutgen *et al.*, 2005). More recently, the FOV of PETIS has been increased to roughly 14 cm × 21 cm (Kawachi *et al.*, 2006). In addition, the Institute of Chemistry and Dynamics of the Geosphere Phytosphere research group in Germany has developed a three-dimensional (3D) imaging system for plant studies, the Plant Tomographic Imaging System or PlanTIS (Streun *et al.*, 2007). The PlanTIS device has a cylindrical geometry that provides 1.3 mm resolution with an axial FOV of about 11 cm (Streun *et al.*, 2006, 2007).

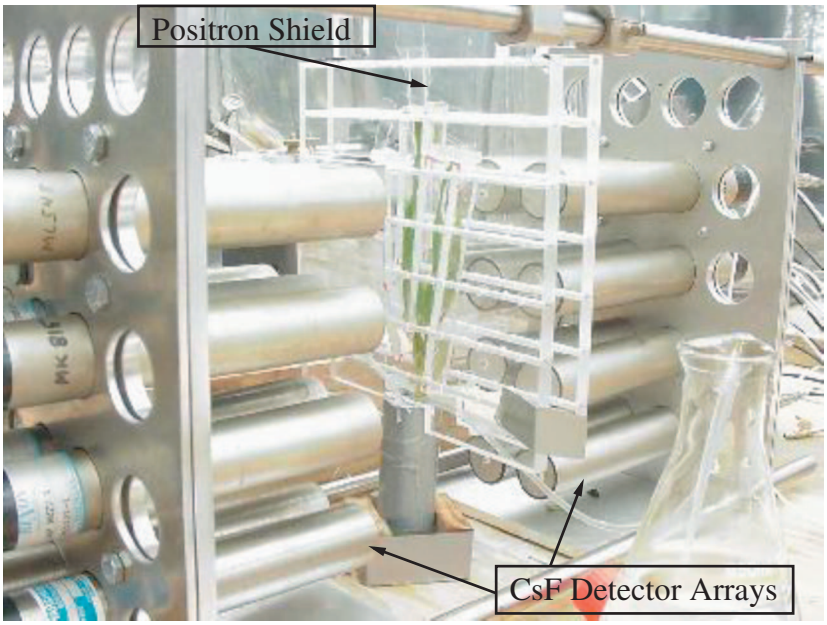

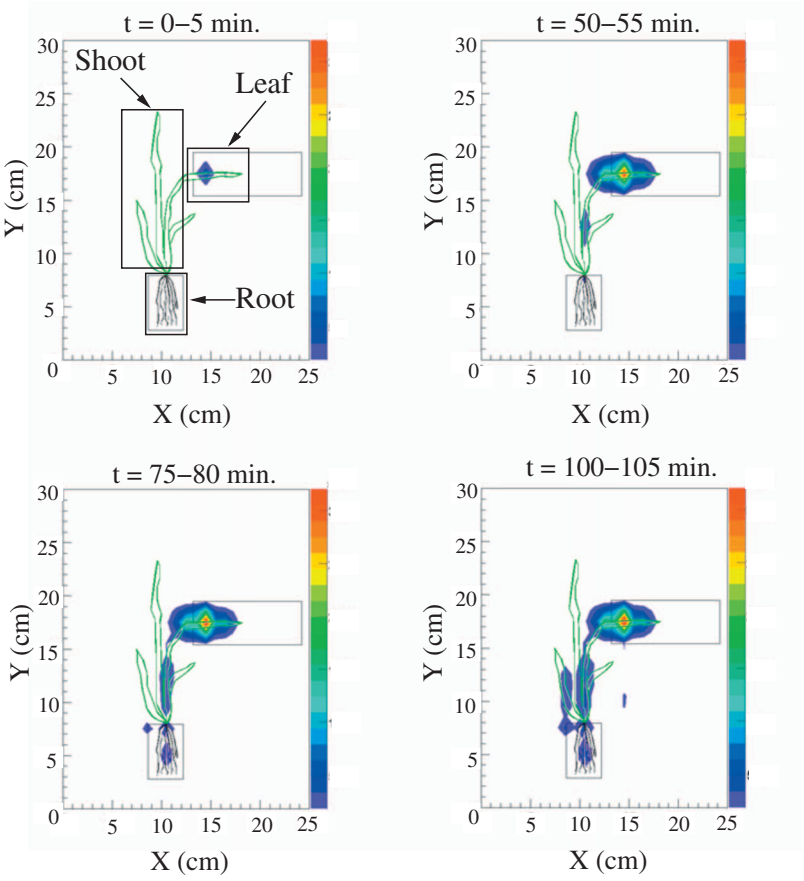

Figure 3. (Above) Photograph of a barley plant arranged within the FOV of the low spatial resolution 2D PET imager. Each detector cylinder is a cesium fluoride scintillator with dimensions 25 mm diameter by 45 mm thick. A plastic shield equipped with ventillation ducts is placed near the plant surface to stop positrons that escape from the plant tissue so that they annihilate within the imager FOV. Individual barley leaves are also separated with plastic shields to ensure that positron annihilation occurs locally. (Below) Snapshots indicating ^{11}C-labeled photoassimilate accumulation in a barley plant as a function of time. The integration time for these images is 5 min; the minimum exposure time is imposed by the counting rate of the detector system and the minimum required counting statistics within each region of interest. The relative intensity of the source in the image plane is coded according to the color scale on the right side of each frame with red representing the brightest pixels. The images are corrected for background radiation, radioactive decay of ^{11}C, and the detection efficiency as a function of location in the image plane. In the first frame (0–5 min), the regions of interest (leaf, shoot, and root, as indicated by the rectangular boxes) are selected for direct comparison to earlier collimated detector measurements.

The Duke prototype PET imager has been used to measure allocation of ^{11}C-labeled photoassimilates in small plants for studies examining limitations of photoassimilate export in elevated CO_2 environments. The uptake leaf, shoot, and roots are all visible within the detector FOV, thereby enabling coherent tracing of ^{11}C throughout an entire plant. Images are reconstructed by integrating the events accumulated during a specific exposure time. For example, the images

shown in Fig. 3 are 5-min-long exposures. The duration of each exposure is limited to the time required to yield a statistically significant number of detected events from each region of interest. This integration time can be adjusted to provide finer temporal resolution as long as the counting statistics for each region of interest remain adequate. The counting statistics can be improved by moving the detector arrays closer together, increasing the initial ^{11}C activity, or selecting larger regions of interest. While the spatial resolution of the instrument is fixed by the detector geometry, the temporal resolution can vary depending on the particular application but is fundamentally limited by the time-stamp clock frequency.

Determination of ^{11}C profiles using PET-based methods requires image construction from raw coincidence event data. The analysis involves ray tracing to determine the location of the event vertex and correcting the raw data for geometric and gamma-ray detection efficiencies using Monte Carlo simulations of the imager-plant setup. These analysis techniques are well proven and comparisons of simulations to independent benchmark data for a particular experimental setup provide checks for implementation mistakes and assessments of systematic errors. We used the results of collimated single-detector measurements as the standard to which our PET-based data were compared. The single-detector method was chosen as the standard because it measures ^{11}C profiles directly, i.e., without the complexities of event reconstruction. Verification of the PET-based measurement techniques using single-detector benchmark data was carried out in two steps.

First, collimation techniques were used to determine carbon allocation on a coarse spatial scale by measuring ^{11}C accumulation in three regions of barley (*Hordeum distichum L.*) plants: the uptake leaf, the shoot, and the root. Barley plants were chosen because of their successful use in previous radiotracer studies of carbon transport and allocation (e.g., Thorpe and Minchin, 1991). Each region was viewed by a single collimated bismuth germanate (BGO) detector. The collimators were made of small lead shielding blocks that were arranged to define the FOV of each detector to a specific region of the plant. This detector arrangement is commonly used for ^{11}C-labeled photoassimilate tracking (Minchin and Thorpe, 2003; Schwachtje *et al.*, 2006) and gives results with only minor processing of the raw data. Because only one of the emitted gamma rays from electron-positron annihilation in the plant tissue is detected, each region of interest is defined solely by the geometry of the lead shielding. Tracer profiles from the collimated detector measurements were analyzed using an input-output statistical model (Minchin, 1978). The physical parameters that result from this analysis are the system gain (fraction of the input that arrives at the output) and the average transit time, which is used to calculate the average photoassimilate velocity (Minchin and Troughton, 1980). With our detection system, both leaf and shoot exports were evaluated, thereby enabling the determination of the fraction of ^{11}C allocated to each section of the plant (partitioning fraction).

Second, results from the event reconstruction and analysis of data taken with our 2D imager were compared with data obtained from the collimated single-detector measurements that were made as described above. The imaging measurements were made on barley plants similar in age and growth conditions as those used in the collimation experiments. The barley seedlings were labeled with $^{11}CO_2$, and the ^{11}C-photoassimilates were tracked throughout the entire plant using the low resolution prototype imager. To enable direct comparisons between the results obtained with the two techniques the regions of interest within the imager FOV were chosen to match the regions measured in the collimated detector experiments. Time series snapshots with exposure times of 5 min, as shown in Fig. 3, were used to trace the accumulation of ^{11}C in the barley seedlings. The regions of interest, which are the uptake leaf, the shoot, and the root, are indicated by the rectangles in the first image frame. Tracer profiles for each region of interest are generated by integrating the image pixel values within the region for all corrected exposure images. The input-output statistical model was applied to the tracer profiles obtained from the image data to provide information about leaf and shoot export. The leaf export analysis quantifies the flow of photoassimilate out of the uptake leaf and into the shoot and roots. Similarly, the shoot export analysis describes the flow of radiotracer from the shoot to the roots. The statistical input-output methods were developed for use with individual detectors collimated to monitor photoassimilate accumulation in terminal sinks of the plant as well as the entire organism. However, these same techniques can be applied to 2D PET images without gaps between the detection regions as is often the case in collimated detector measurements; electronic definition of the region of interest and integration of pixels in the 2D images enables spatial continuity in the substance flow analysis. The advantages of the imaging technique are improved spatial resolution and the ability to quantify radiotracer flow between any physiologically relevant regions of interest in the image plane. The application of input-output modeling to tracer profiles from 2D PET images has previously been demonstrated with PETIS (Keutgen *et al.*, 2002;Keutgen *et al.*, 2005; Matsuhashi *et al.*, 2005).

The patterns of carbon partitioning obtained from the measurements made with the prototype 2D PET imager are consistent with the results from our collimated detector measurements (Table II), thus validating the image reconstruction and analysis techniques applied to the 2D PET imaging data. Uncertainties in the partitioning fractions determined from our collimated detector data are primarily due to variations within an individual plant as was assessed by labeling the same plant multiple times. The somewhat larger errors in the partitioning fractions determined using the 2D PET

Table II. Comparison of the results of our carbon partitioning measurements made using collimated detection to those obtained with our prototype 2D PET system. Both measurement methods were applied on barley seedlings that were 10–12 days old. These seedlings were grown and labeled at a CO_2 concentration of 350 ppm. The errors in the measured quantities are mostly due to systematic uncertainties. In both methods the statistical uncertainties were generally a factor of 10 smaller than the systematic errors.

Measurement method	Labeled leaf fraction	Shoot fraction	Root fraction
Collimated detectors	0.35±0.02	0.45±0.04	0.20±0.03
Prototype 2D PET	0.34±0.10	0.52±0.08	0.14±0.03

imager reflect both variation within an individual plant and differences between plants; the PET-based data were accumulated using several plants, not just one as was used in the collimated detector measurements.

High spatial resolution 2D PET imaging: VIPER

The 2D PET imaging technique is applicable to a broad range of spatial scales with the achievable spatial resolution mostly dependent on the size of the individual detector elements. A high spatial resolution 2D PET imager composed of two 5 cm×5 cm detector modules was designed at Duke University to provide greater spatial detail. Each module consists of a planar array of pixelated BGO crystals (15×15) coupled to a position-sensitive photomultiplier tube (PSPMT) with the associated position calculating circuitry. The dimensions of each BGO pixel are 3 mm (wide) ×3 mm (high) ×25 mm (thick), and adjacent pixels are optically decoupled by a 0.25-mm-thick reflective material. These crystals are coupled to a PSPMT with 8×8 anode pads and an active area of 49 mm×49 mm. To reduce the number of analog-to-digital conversion channels required for BGO pixel identification within each module, position-calculating circuit boards are mounted onto the PSPMT. This arrangement reduces the number of readout channels for each module from 64 (8×8) anode signals to four position signals (X_+, X_-, Y_+, and Y_-) (Popov *et al.*, 2001). Because the modular design of this system makes it highly adaptable to a wide variety of geometries in plant studies, we refer to it to as the Versatile Imager for Positron Emitting Radiotracers (VIPER).

The Duke VIPER is similar to the PETIS instrument that was developed at the Japan Atomic Energy Research Institute. Both devices have a FOV of approximately 5 cm×5 cm, although the PETIS imager employs finer scintillator segmentation (2 mm×2 mm×20 mm BGO scintillator pixels). The PETIS was recently used to visualize the accumulation of photoassimilates in grains of a wheat ear (Matsuhashi *et al.*, 2006) with 2.3 mm resolution. Finer detector segmentation can provide better spatial resolution in an ideal situation, although the actual spatial resolution is generally degraded by positron range effects. For positrons emitted by ^{11}C decay in wet tissue, the average distance the positron travels before annihilation is about a millimeter. However, positrons near the surface of the plant may escape and travel up to 4 m in air before annihilating. To ensure positron annihilation as close to the decaying ^{11}C nucleus as possible, a plastic shield is placed near the surface of the plant to supply an annihilation medium (Minchin and Thorpe, 2003). The plastic shield increases detection efficiency since positrons that could have otherwise escaped are stopped within the detection FOV. However, overall spatial resolution is degraded due to the increased distance allowed between the location of the ^{11}C nucleus and the site of electron-positron annihilation. This trade-off between the efficiency for detecting the positron annihilations and spatial resolution is required to ensure that all positrons emitted within the FOV are accurately counted.

The capabilities of the VIPER have been demonstrated using both ^{11}C and ^{13}N radiotracers. The ability to measure carbon accumulation as a function of position within the VIPER FOV was demonstrated by tracking the distribution of ^{11}C-labeled photoassimilates in a 5 cm×5 cm region of a germinated bean (*Pisum sativum L.*) seedling (Fig. 4). In these measurements the labeled leaf was sealed in a cuvette into which air with a mixture of $^{12}CO_2$ and $^{11}CO_2$ flowed. The labeling cuvette was located above the imager FOV and the roots were placed in a hydroponic rectangular container. For the images shown in Fig. 4, the FOV of the VIPER included the shoot and the upper portion of the roots. The integration time for each frame in Fig. 4 was 5 min. Note that tracer accumulation is first detected in the lower shoot region about 25 min after $^{11}CO_2$ is introduced to the labeled leaf. This delay is the time required for $^{11}CO_2$ assimilation in the leaf and the subsequent transport of photoassimilates out of the leaf and through the upper portion of the shoot. The ^{11}C-labeled carbohydrates are then transported around the seed cotyledon and down into the upper root region. Though most of the ^{11}C accumulation is observed in the primary root possibly for storage, significant accumulation is measured in a fine root after about 80 min of labeling (seen just to the left of the bubbling tube in Fig. 4) suggesting lower C allocation priorities in the fine active roots. The series of images demonstrates the ability of the VIPER to reconstruct the distribution of ^{11}C-labeled photoassimilates with high spatial resolution in a 5 cm×5 cm FOV.

Measurement of transport properties in the translocation of nitrogen ions from the root bathing solution to the foliage of a barley plant has also been carried out successfully with the VIPER. Here, nitrate ions ($^{13}NO_3^-$) were produced at TUNL by bombarding a depleted water target (H_2O with 99.99% ^{16}O) with a proton beam. This process results in an aqueous solution of ^{13}N nuclei that are >90% $^{13}NO_3^-$. Nitrite and ammonium ions are also produced in the solution in small quantities (Chasko and Thayer, 1981). The ^{13}N-labeled

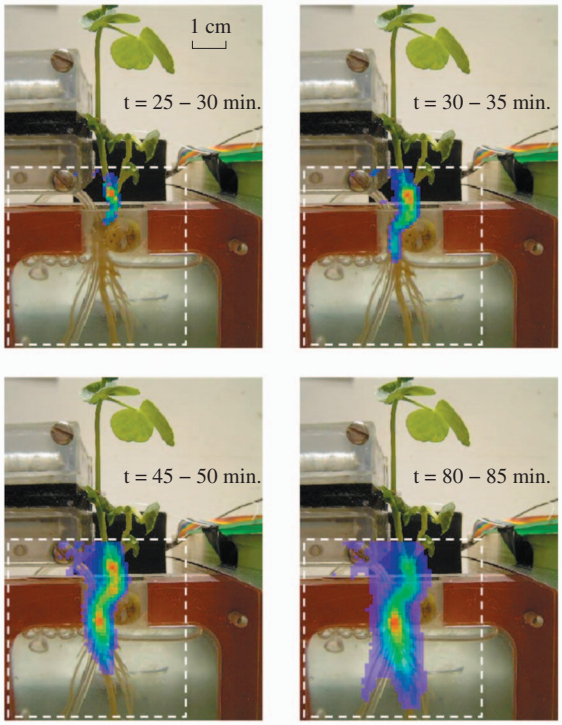

Figure 4. Snapshots taken with VIPER of accumulation of ^{11}C-labeled photoassimilates in the lower shoot and root of a bean plant as a function of time. The images are obtained by coincidence detection of the back-to-back gamma rays emitted from positron annihilation in the plant. The dashed square indicates the VIPER FOV, and each image pixel is 1 mm × 1 mm. The integration time for these images is 5 min for demonstration purposes, but the exposure time can be decreased to 1 min, which is the limit imposed by the counting statistics within each region of interest for this particular setup.

solution was added to the root hydroponic solution, and ^{13}N-labeled ions were assimilated in the roots and transported to plant sinks. The ^{13}N in the roots was monitored using coincidence counting, and the VIPER was used to visualize ^{13}N accumulation in two leaves of a barley plant. After about 15 min the ^{13}N-labeled compounds were detected in leaves located about 6 cm above the shoot-root interface (data not shown).

Hybrid detection system with low and high spatial resolution techniques

The integration of coincidence counting with high resolution 2D PET imaging is an efficient and effective approach to studying entire plants and plant systems where a large or distributed FOV is required. The types of experiments that can currently be performed with high spatial resolution are primarily limited by the FOV covered by imaging devices with resolution finer than about 3 mm. Though high spatial resolution is desired in many instances, some regions of interest for the overall analysis may not require detailed spatial information. These regions can be monitored separately using coincidence counting with nonsegmented detectors.

Combining high spatial resolution imaging with coincidence counting to form a hybrid radiotracer system requires an accurate determination of the relative detection efficiency for each detection region. The relative detection efficiency for each region of our hybrid system is determined by placing a positron-emitting source at the center of each FOV and measuring the decay-corrected count rate. The positron-emitting source is a granule of soda lime that has absorbed $^{11}CO_2$ gas. Monte-Carlo simulations are used to calculate the relative detection efficiency as a function of position across each FOV. The simulation for the VIPER is normalized to the efficiency of the other detector pairs in the system using the measurements made with the soda-lime source. For regions monitored by nonsegmented detectors, the measured relative detection efficiency is scaled by the average calculated detection efficiency across the FOV. Once corrections for background radiation, radioactive half-life, and relative detection efficiency have been applied, quantitative determinations of material flow throughout the entire system can be made.

An example of experiments being performed at Duke University that takes advantage of a hybrid detection system is the measurement of total carbon allocation and translocation, including root exudation and root respiration under various environmental conditions. Coincidence counting is utilized to monitor accumulation of ^{11}C-photoassimilates in the labeled leaf and roots; it is also used to monitor the exudation of soluble ^{11}C-labeled compounds from the roots and $^{11}CO_2$ gas that is respired by the roots. The quantity of radiotracer released from plant roots in the form of soluble exudates or respired carbon dioxide gas is measured by circulating the root bathing solution in a closed system (Fig. 5). The flow of the circulated solution transports soluble exudates out of the rhizosphere and into a flask where a detector monitors radiotracer accumulation within a sample of the well-mixed solution. This experimental design is a modification of the setup used by Minchin and McNaughton (1984). While high spatial resolution imaging is not required to monitor the root exudation and respiration flasks, it is needed in the shoot region to enable measurement of material flow in regions of interest within the shoot as well as carbon allocation analysis on a coarse spatial scale (i.e., leaf, shoot, and root). Better spatial resolution can elucidate relative sink strengths, such as reloading of photoassimilate into a region of the shoot adjacent to the labeled leaf rather than root allocation.

FUTURE DIRECTIONS

To coherently trace short-lived positron-emitting isotopes throughout an entire plant seedling or parts of a larger plant with high spatial resolution, detector modules similar to the ones in the current small FOV imagers can be tiled into planar arrays. This concept has driven the development of a large FOV imager at Duke based on tiled arrays of the VIPER module. The proposed imager is composed of 4 × 6 detector modules in each array, covering a FOV approxi-

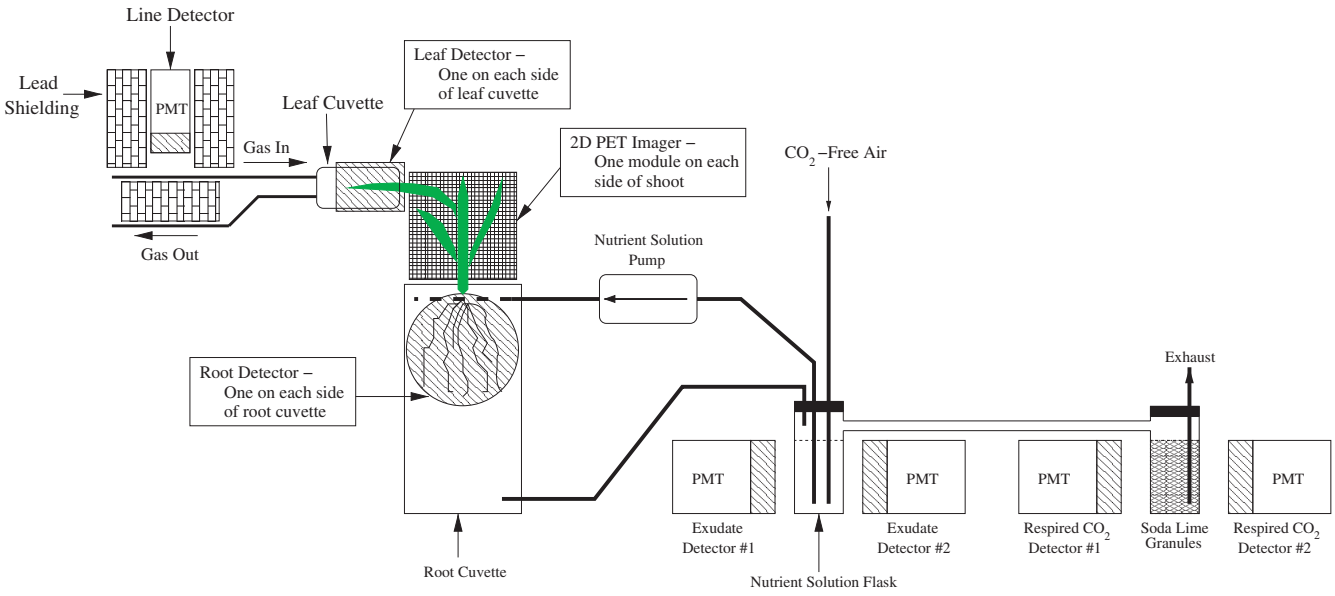

Figure 5. Diagram of an experiment that uses the hybrid detector system to measure full-plant carbon partitioning dynamics as well as root exudation and root respiration. The root exudation and respiration are measured by circulating the root bathing solution in a closed loop. The ^{11}C accumulation in the labeled leaf and root is monitored via coincidence counting instead of imaging because high spatial resolution is not required in these regions. Coincidence counting is also used to monitor ^{11}C-labeled root exudates and $^{11}CO_2$ respired from the roots. VIPER is used to measure ^{11}C accumulation in the shoot of the plant.

mately 20 cm wide ×30 cm tall. The primary benefit of this modular design is the flexibility it provides. The modules may be rearranged within the detector array frame to accommodate various plant geometries while covering a total imaging area of 600 cm^2. This type of flexibility is not a standard feature of commercially available PET imaging devices. Hamamatsu Photonics has constructed and demonstrated the capabilities of an imaging system with a FOV approximately 12 cm wide ×19 cm tall and a spatial resolution of 2 mm (Uchida *et al.*, 2004; Kawachi *et al.*, 2006), and PlanTIS provides 3D images with a spatial resolution of 1.3 mm (Streun *et al.*, 2007). Though these systems currently have the largest coverage areas of any high spatial resolution PET imaging systems with demonstrated plant applications, they do not offer the flexibility of the planned Duke imager.

Imaging and quantitative analysis of the dynamic transport of metabolites using radiotracers will improve our understanding of the complexity of controls on plant growth and development in changing environments. Measurement of radiotracer transport and allocation over a large FOV with high spatial resolution will provide information on fine-scale dynamics that is not accessible using other techniques. For example, characterization of gene function for whole-plant transgenics can be monitored in dynamic light environments, in soils with heterogeneous nutrient availability or water pulses, or after insect or pathogen attacks. The technique can be used for screening different genotypes for particular traits likely to improve plant growth. Additionally, imaging techniques will provide data to parameterize and test plant growth models from the plant-soil interface (e.g., root exudates-microbe interactions) to the physiological limitations of source-sink carbohydrate loading in future elevated CO_2 environment or in polluted air, whole-plant dynamics of carbon allocation as mediated by nitrogen, and whole-plant hydraulics in fluctuating environments. The variety of plants species used and their different growth stages requires a versatile imaging system made up of both high and low spatial resolution components that provides the opportunity to observe the spatiotemporal dynamics of metabolites on multiple scales. In addition to providing physiological information, versatile radiotracer imaging systems can also be used to provide a better understanding of metabolite dynamics on an ecological scale, such as insight into plant-fungal interactions or responses to herbivory.

CONCLUSIONS

The collaboration of scientists across multiple disciplines provides the expertise to study the responses of plants to environmental changes using radioisotopes. Measurements with short-lived positron-emitting isotopes have led to a better understanding of basic physiological and ecological phenomena. The development of quantitative analysis methods for tracer profiles has been crucial to the interpretation of measurements using short-lived radioisotopes. Statistical input-output models do not require *a priori* knowledge of the mechanisms driving tracer transport, but physiologically meaningful parameters can be determined from data using this model, thereby providing consistency checks on mechanistic interpretations of certain phenomena. The recent application of PET techniques for plant research allows for obser-

vation of real-time metabolite dynamics on previously unexplored spatial scales and creates opportunities for new discoveries. At the subcellular scale, the increased knowledge of genomes for various species combined with the spatio-temporal measurements made possible by new radiotracer techniques could help identify gene function in an environmental context. At the other end of the spatial scale, i.e., plant-organism interactions, the technique has promise in helping to elucidate the dynamics of short-term energy and nutrient fluxes between organisms.

ACKNOWLEDGMENTS

We would like to thank anonymous reviewers for their insightful and constructive feedback. Thank you to Peter Minchin for helping us get started with short-lived positron emitting radiotracer labeling. Also, many thanks to Stan Majewski and the Detector and Imaging Group at Jefferson Lab for providing the position calculation circuit boards for the prototype VIPER imager and to Emily Bernhardt for her insightful suggestions during the early stages of this collaboration. Thank you as well to Todd Smith at the Phytotron and Bret Carlin, John Dunham, David Hoyt, Patrick Mulkey, Richard O'Quinn, and Chris Westerfeldt at TUNL for their technical assistance. Funding for this research is provided by the US Department of Energy (DOE), Office of Nuclear Physics, Grant No. DE-FG02-97ER41033 (TUNL), the National Science Foundation (NSF), Grant No. IBN-9985877 (Phytotron), and the NSF, Grant No. DBI-0649924.

REFERENCES

Ananyev, G, Kolber, ZS, Klimov, D, Falkowski, PG, Berry, JA, Rascher, U, Martin, R, and Osmond, B (2005). "Remote sensing of heterogeneity in photosynthetic efficiency, electron transport and dissipation of excess light in *Populus deltoides* stands under ambient and elevated CO_2 concentrations, and in a tropical forest canopy, using a new laser-induced fluorescence transient device." *Glob. Chang. Biol.* **11**, 1195–1206.

Babst, AB, Ferrieri, RA, Gray, DW, Lerdau, M, Schlyer, DJ, Schueller, M, Thorpe, MR, and Orians, CM (2005). "Jasmonic acid induces rapid changes in carbon transport and partitioning in *Populus*." *New Phytol.* **167**, 63–72.

Bailey, DL, Carp, JS, and Surti, S (2003). *Positron Emission Tomography: Basic Science and Clinical Practice*, pp 41–67, Springer-Verlag, London.

Bancal, P, and Soltani, F (2002). "Source-sink partitioning. Do we need Münch?" *J. Exp. Bot.* **53**, 1919–1928.

Bishop, HT, Thompson, RG, Aikman, DP, and Fensom, DS (1986). "Fine structure aberrations in the movement of ^{11}C and ^{13}N in the stems of plants." *J. Exp. Bot.* **37**, 1780–1794.

Brady, SM, Orlando, DA, Lee, J, Wang, JY, Koch, J, Dinneny, JR, Mace, D, Ohler, U, and Benfey, PN (2007). "A high-resolution root spatiotemporal map reveals dominant gene expression patterns." *Science* **318**, 801–806.

Britto, DT, and Kronzucker, HJ (2003). "Trans-stimulation of $^{13}NH_4^+$ efflux provides evidence for the cytosolic origin of tracer in the compartmental analysis of barley roots." *Functional Plant Bio.* **30**, 1233–1238.

Britto, DT, Siddiqi, MY, Glass, ADM, and Kronzucker, HJ (2002). "Subcellular NH_4^+ flux analysis in leaf segments of wheat (*Triticum aestivum*)." *New Phytol.* **155**, 373–380.

Buchwald, P, and Sveiczer, A (2006). "The time-profile of cell growth in fission yeast: model selection criteria favoring bilinear models over exponential ones." *Theoretical Biology and Medical Modelling*, **3**, 16–25.

Cadzow, JA (1973). *Discrete-Time Systems*, Prentice-Hall, Englewood Cliffs, NJ.

Caldwell, CD, Fensom, DS, Bordeleau, L, Thompson, RG, Drouin, R, and Didsbury, R (1984). "Translocation of ^{13}N and ^{11}C between nodulated roots and leaves in alfalfa seedlings." *J. Exp. Bot.* **35**, 431–443.

Chasko, JH, and Thayer, JR (1981). "Rapid concentration and purification of ^{13}N-labelled anions on a high performance anion exchanger." *Int. J. Appl. Radiat. Isot.* **32**, 645–649.

Chatziioannou, AF (2002). "PET scanners dedicated to molecular imaging of small animal models." *Mol. Imaging Biol.* **4**, 47–63.

Chavarria-Krauser, A, Nagel, KA, Palme, K, Schurr, U, Walter, A, and Scharr, H (2008). "Spatio-temporal quantification of differential growth processes in root growth zones based on a novel combination of image sequence processing and refined concepts describing curvature production." *New Phytol.* **177**, 811–821.

Chen, DX, and Coughenour, MB (2004). "Photosynthesis, transpiration, and primary productivity: scaling up from leaves to canopies and regions using process models and remotely sensed data." *Global Biogeochem. Cycles* **18**, GB4033.

Cherry, S, *et al.* (1997). "MicroPET: a high resolution PET scanner for imaging small animals." *IEEE Trans. Nucl. Sci.* **44**, 1161–1166.

Daudet, FA, Lacointe, A, Gaudillere, JP, and Cruiziat, P (2002). "Generalized Münch coupling between sugar and water fluxes for modeling carbon allocation as affected by water status." *J. Theor. Biol.* **214**, 481–498.

Dyer, MI, Acra, MA, Wang, GM, Coleman, DC, Freckman, DW, McNaughton, SJ, and Strain, BR (1991). "Source-sink carbon relations in two *Panicum coloratum* ecotypes in response to herbivory." *Ecology* **72**, 1472–1483.

Fares, Y, Goeschl, JD, Magnuson, CE, Scheld, HW, and Strain, BR (1988). "Tracer kinetics of plants carbon allocation with continuously produced $^{11}CO_2$." *J. Radioanal. Nucl. Chem.* **124**, 105–122.

Farquhar, GD, Caemmerer, SV, and Berry, JA (1980). "A biochemical model of photosynthetic CO_2 assimilation in leaves of C-3 species." *Planta* **149**, 78–90.

Farquhar, GD, O'Leary, MH, and Berry, JA (1982). "On the relationship between carbon isotope discrimination and the intercellular carbon dioxide concentration in leaves." *Aust. J. Plant Physiol.* **9**, 121–137.

Ferrieri, AP, Thorpe, MR, and Ferrieri, RA (2006). "Stimulating natural defenses in poplar clones (OP-367) increases plant metabolism of carbon tetrachloride." *Int. J. Phytoremediation* **8**, 233–243.

Ferrieri, RA, Gray, DW, Babst, BA, Schueller, MJ, Schlyer, DJ, Thorpe, MR, Orians, CM, and Lerdau, M (2005). "Use of carbon-11 in *Populus* shows that exogenous jasmonic acid increases biosynthesis of isoprene from recently fixed carbon." *Plant, Cell Environ.* **25**, 591–602.

Field, CB, Randerson, JT, and Malmström, CM (1995). "Global net primary production: combining ecology and remote sensing." *Remote Sens. Environ.* **51**, 74–88.

Fischlin, A, Midgley, GF, Price, JT, Leemans, R, Gopai, B, Turley, C, Rounsevell, MDA, Dube, OP, Tarazone, J, and Velichko, AA (2007). "Ecosystems, their properties, goods, and services." In *Climate Change 2007: Impacts, Adaptation and Vulnerability*, Parry, ML, Canziani, OF, Palutikof, JP, van der Linden, PJ, and Hanson, CE (eds.) pp 211–272, Cambridge University Press, Cambridge.

Freckman, DW, Barker, KR, Coleman, DC, Acra, M, Dyer, MI, Strain, BR, and McNaughton, SJ (1991). "The use of the ^{11}C technique to measure plant responses to herbivorous soil nematodes." *Funct. Ecol.* **5**, 810–818.

Fritz, E, Evert, RF, and Heyser, W (1983). "Microautoradiographic studies of phloem loading and transport in the leaf of *Zea mays L.*" *Planta* **159**, 193–206.

Gest, H (2005). "Samuel Ruben's contributions to research on photosynthesis and bacterial metabolism with radioactive carbon." In *Discoveries in Photosynthesis*, Govindjee, Beatty, JT, Gest, H, and Allen, JF (eds.) pp 131–137, Springer, Dordrecht, The Netherlands.

Glass, ADM, Thompson, RG, and Bordeleau, L (1985). "Regulation of NO_3^- influx in barley." *Plant Physiol.* **77**, 379–381.
Goeschl, JD, Magnuson, CE, DeMichele, DW, and Sharpe, PJH (1976). "Concentration-dependent unloading as a necessary assumption for a closed form mathematical model of osmotically driven pressure flow in phloem." *Plant Physiol.* **58**, 556–562.
Grodzinski, B, Jahnke, S, and Thompson, R (1984). "Translocation profiles of [^{11}C] and [^{13}N]-labeled metabolites after assimilation of $^{11}CO_2$ and [^{13}N]-labeled ammonia gas by leaves of *Helianthus annuus L.* and *Lupinus albus L.*" *J. Exp. Bot.* **35**, 678–690.
Haustein, E, and Schwille, P (2007). "Trends in fluorescence imaging and related techniques to unravel biological information." *HFSP J.* **1**, 169–180.
Himmelbach, A, Iten, M, and Grill, E (1998). "Signaling of abscisic acid to regulate plant growth." *Philos. Trans. R. Soc. London, Ser. B* **353**, 1439–1444.
Jahnke, S, Stöcklin, G, and Willenbrink, J (1981). "Translocation profiles of ^{11}C-assimilates in the petiole of *Marsilea quadrifolia* L." *Planta* **153**, 56–63.
Jones, HG, and Morison, J (eds.) (2007). "Imaging techniques for understanding plant responses to stress." *J. Exp. Bot.* **58**(4), 743–898.
Kaestner, A, Schneebeli, M, and Graf, F (2006). "Visualizing three-dimensional root networks using computed tomography." *Geoderma* **136**, 459–469.
Kawachi, N, Sakamoto, K, Ishii, S, Fujimaki, S, Suzui, N, Ishioka, NS, and Matsuhashi, S (2006). "Kinetic analysis of carbon-11-labeled carbon dioxide for studying photosynthesis in a leaf using positron emitting tracer imaging system." *IEEE Trans. Nucl. Sci.* **53**, 2991–2997.
Keutgen, AJ, *et al.* (2005). "Input-output analysis of *in vivo* photoassimilate translocation using positron-emitting tracer imaging system (PETIS) data." *J. Exp. Bot.* **56**, 1419–1425.
Keutgen, N, *et al.* (2002). "Transfer function analysis of positron-emitting tracer imaging system (PETIS) data." *Appl. Radiat. Isot.* **57**, 225–233.
Kiyomiya, S, *et al.* (2001a). "Light activates $H_2^{15}O$ flow in rice: detailed monitoring using a positron-emitting tracer imaging system (PETIS)." *Physiol. Plant.* **113**, 359–367.
Kiyomiya, S, *et al.* (2001b). "Real time visualization of ^{13}N-translocation in rice under different environmental conditions using positron emitting tracer imaging system." *Plant Physiol.* **125**, 1743–1754.
Kronzucker, HJ, Glass, ADM, and Siddiqi, MY (1995a). "Nitrate induction in spruce: an approach using compartmental analysis." *Planta* **196**, 683–690.
Kronzucker, HJ, Guy, GUD, Siddiqi, MY, and Glass, ADM (1998). "Effects of hypoxia on $^{13}NH_4^+$ fluxes in rice roots." *Plant Physiol.* **116**, 581–587.
Kronzucker, HJ, Siddiqi, MY, and Glass, ADM (1995b). "Compartmentation and flux characteristics of nitrate in spruce." *Planta* **196**, 674–682.
Kronzucker, HJ, Siddiqi, MY, and Glass, ADM (1995c). "Compartmentation and flux characteristics of ammonium in spruce." *Planta* **196**, 691–698.
Kronzucker, HJ, Siddiqi, MY, and Glass, ADM (1995d). "Analysis of $^{13}NH_4^+$ efflux in spruce roots." *Plant Physiol.* **109**, 481–490.
Kume, T, *et al.* (1997). "Uptake and transport of positron-emitting tracer ^{18}F in plants." *Appl. Radiat. Isot.* **48**, 1035–1043.
Lapinskas, PJ, Cunningham, KW, Liu, XF, Fink, GR, and Culotta, C (1995). "Mutations in PMR1 suppress oxidative damage in yeast-cells lacking superoxide-dismutase." *Mol. Cell. Biol.* **15**, 1382–1388.
Lee, RB, and Clarkson, DT (1986). "Nitrogen-13 studies of nitrate fluxes in barley roots: I. Compartmental analysis from measurements of ^{13}N efflux." *J. Exp. Bot.* **37**, 1753–1767.
Lee, RB, and Drew, MC (1986). "Nitrogen-13 studies of nitrate fluxes in barley roots: II. Effect of plant N-status on the kinetic parameters of nitrate influx." *J. Exp. Bot.* **37**, 1768–1779.
Lough, TJ, and Lucas, WJ (2006). "Integrative plant biology: role of phloem long-distance macromolecular trafficking." *Annu. Rev. Plant Biol.* **57**, 203–232.
MacFall, JS, Johnson, GA, and Kramer, PJ (1990). "Observation of a water-depletion region surrounding loblolly pine roots by magnetic resonance imaging." *Proc. Natl. Acad. Sci. U.S.A.* **87**, 1203–1207.
Magnuson, CE, Fares, Y, Goeschl, JD, Nelson, CE, Strain, BR, Jaeger, CH, and Bilpuch, EG (1982). "An integrated tracer kinetics system for studying carbon uptake and allocation in plants using continuously produced $^{11}CO_2$." *Radiat. Environ. Biophys.* **21**, 51–65.
Margolis, HA, Delaney, S, Vezina, LP, and Bellefleur, P (1991). "The partitioning of ^{14}C between growth and differentiation within stem-deformed and healthy black spruce seedlings." *Can. J. Bot.* **69**, 1225–1231.
Matsuhashi, S, *et al.* (2006). "A new visualization technique for the study of the accumulation of photoassimilates in wheat grains using [^{11}C]CO_2." *Appl. Radiat. Isot.* **64**, 435–440.
Matsuhashi, S, Fujimaki, S, Kawachi, N, Sakamoto, K, Ishioka, N, and Kume, T (2005). "Quantitative modeling of photoassimilate flow in an intact plant using the positron emitting tracer imaging system (PETIS)." *Soil Sci. Plant Nutrition* **51**, 417–423.
McKinney, CJ, Fares, Y, Musser, RL, Goeschl, JD, Magnuson, CE, and Need, JL (1989). "Transportation system for $^{11}CO_2$." *Rev. Sci. Instrum.* **60**, 783–786.
McNaughton, GS, and Presland, MR (1983). "Whole plant studies using radioactive 13-Nitrogen: I." *J. Exp. Bot.* **34**, 880–892.
Minchin, PEH (1978). "Analysis of tracer profiles with applications to phloem transport." *J. Exp. Bot.* **29**, 1441–1450.
Minchin, PEH, Farrar, J, and Thorpe, MR (1994). "Partitioning of carbon in split root systems of barley: effect of temperature of the root." *J. Exp. Bot.* **45**, 1103–1109.
Minchin, PEH, and Grusak, MA (1988). "Continuous *in vivo* measurement of carbon partitioning within whole plants." *J. Exp. Bot.* **39**, 561–571.
Minchin, PEH, and Lacointe, A (2005). "New understanding on phloem physiology and possible consequences for modeling long-distance carbon transport." *New Phytol.* **166**, 771–779.
Minchin, PEH, and McNaughton, G (1984). "Exudation of recently fixed carbon by non-sterile roots." *J. Exp. Bot.* **35**, 74–82.
Minchin, PEH, and Thorpe, MR (1987). "Measurement of unloading and reloading of photo-assimilate within the stem of bean." *J. Exp. Bot.* **38**, 211–220.
Minchin, PEH, and Thorpe, MR (1989). "Carbon partitioning to whole versus surgically modified ovules of pea: an application of the *in vivo* measurement of carbon flows over many hours using the short-lived isotope carbon-11." *J. Exp. Bot.* **40**, 781–787.
Minchin, PEH, and Thorpe, MR (2003). "Using the short-lived isotope ^{11}C in mechanistic studies of photosynthate transport." *Functional Plant Biol.* **30**, 831–841.
Minchin, PEH, Thorpe, MR, and Farrar, JF (1993). "A simple mechanistic model of phloem transport which explains sink priority." *J. Exp. Bot.* **44**, 947–955.
Minchin, PEH, Thorpe, MR, Wünsche, J, Palmer, J, and Picton, R (1997). "Carbon partitioning between apple fruits: short- and long-term response to availability of photosynthate." *J. Exp. Bot.* **48**, 1401–1406.
Minchin, PEH, and Troughton, J (1980). "Quantitative interpretation of phloem translocation data." *Annu. Rev. Plant Physiol.* **31**, 191–215.
Moorby, J, Ebert, M, and Evans, NTS (1963). "The translocation of ^{11}C-labeled photosynthates in the soybean." *J. Exp. Bot.* **14**, 210–220.
Moorby, J, and Jarman, PD (1975). "The use of compartmental analysis in the study of the movement of carbon through leaves." *Planta* **122**, 155–168.
More, RD, and Troughton, JH (1973). "Production of $^{11}CO_2$ for use in plant translocation studies." *Photosynthetica* **7**, 271–274.
Nakanishi, H, *et al.* (1999). "Visualizing real time [11C] methionine translocation in Fe-sufficient and Fe-deficient barley using a positron emitting tracer imaging system (PETIS)." *J. Exp. Bot.* **50**, 637–643.
Nakanishi, T, *et al.* (2001a). "Circadian rhythm in ^{15}O-labeled water uptake manner of a soybean plant by PETIS (Position Emitting Tracer Imaging System)." *Radioisotopes* **50**, 163–168.
Nakanishi, T, *et al.* (2001b). "Comparison of ^{15}O-labeled and ^{18}F-labeled water uptake in a soybean plant by PETIS (Positron Emitting Tracer Imaging System)." *Radioisotopes* **50**, 265–269.
Nakanishi, TM, *et al.* (2001c). "^{18}F used as tracer to study water uptake

and transport imaging of a cowpea plant." *J. Radioanal. Nucl. Chem.* **249**, 503–507.
Nakanishi, TM, Okuni, Y, Furukawa, J, Tanoi, K, Yokota, H, Ikeue, N, Matsubayashi, M, Uchida, H, and Tsiji, A (2003). "Water movement in a plant sample by neutron beam analysis as well as positron emission tracer imaging system." *J. Radioanal. Nucl. Chem.* **255**, 149–153.
Ohtake, N, *et al.* (2001). "Rapid N transport to pods and seeds in N-deficient soybean plants." *J. Exp. Bot.* **52**, 277–283.
Osmond, B, *et al.* (2004). "Changing the way we think about global change research: scaling up in experimental ecosystem science." *Glob. Chang. Biol.* **10**, 393–407.
Osmond, CB (1989). "Photosynthesis from the molecule to the biosphere: a challenge for integration." In *Photosynthesis*, Briggs, WR (ed.) pp 5–17, Alan R. Liss Inc., New York.
Paiva, NL (2000). "An introduction to the biosynthesis of chemicals used in plant-microbe communication." *J. Plant Growth Regulation* **19**, 131–143.
Pickard, W, Minchin, P, and Thorpe, M (1993). "Leaf export and partitioning changes induced by short-term inhibition of phloem transport." *J. Exp. Bot.* **44**, 1491–1496.
Popov, V, Majewski, S, Weisenberger, A, and Wojcik, R (2001). "Analog readout system with charge division type output." *IEEE Nucl. Sci. Symp. Conf. Rec.* **4**, 1937–1940.
Presland, MR, and McNaughton, GS (1984). "Whole plant studies using radioactive 13-nitrogen: II. A compartmental model for the uptake and transport of nitrate ions by *Zea mays*." *J. Exp. Bot.* **35**, 1277–1288.
Presland, MR, and McNaughton, GS (1986). "Whole plant studies using radioactive 13-nitrogen: IV. A compartmental model for the uptake and transport of ammonium ions by *Zea mays*." *J. Exp. Bot.* **37**, 1619–1632.
Reglinski, T, Whitaker, G, Cooney, JM, Taylor, JT, Poole, PR, Roberts, PB, and Kim, KK (2001). "Systematic acquired resistance to *Sclerotinia sclerotiorum* in kiwifruit vines." *Physiol. Mol. Plant Pathol.* **58**, 111–118.
Rieder, CL, and Khodjakov, A (2003). "Mitosis through the microscope: advances in seeing inside live dividing cells." *Science* **300**, 91–96.
Ritchie, RJ (2006). "Estimation of cytoplasmic nitrate and its electrochemical potential in barley roots using $^{13}NO_3^-$ and compartmental analysis." *New Phytol.* **171**, 643–655.
Rohren, EM, Turkington, TG, and Coleman, RE (2004). "Clinical applications of PET in oncology." *Radiology* **231**, 305–332.
Rolland, F, Baena-Gonzalez, E, and Sheen, J (2006). "Sugar sensing and signaling in plants: conserved and novel mechanisms." *Annual Rev. Plant Biol.* **57**, 675–709.
Ruben, S, Hassid, W, and Kamen, M (1939). "Radioactive carbon in the study of photosynthesis." *J. Am. Chem. Soc.* **61**, 661–663.
Sasai, T, Okamoto, K, Hiyama, T, and Yamaguchi, Y (2007). "Comparing terrestrial carbon fluxes from the scale of a flux tower to the global scale." *Ecol. Modell.* **208**, 135–144.
Schmidt, KC, and Smith, CB (2005). "Resolution, sensitivity and precision with autoradiography and small animal positron emission tomography: implications for functional brain imaging in animal research." *Nucl. Med. Biol.* **32**, 719–725.
Schurr, U, Walter, A, and Rascher, U (2006). "Functional dynamics of plant growth and photosynthesis—from steady-state to dynamics—from homogeneity to heterogeneity." *Plant, Cell Environ.* **29**, 340–352.
Schwachtje, J, Minchin, PEH, Jahnke, S, van Dongen, JT, Schittko, U, and Baldwin, IT (2006). "SNF1-related kinases allow plants to tolerate herbivory by allocating carbon to roots." *Proc. Natl. Acad. Sci. U.S.A.* **103**, 12935–12940.
Siddiqi, MY, Glass, ADM, and Ruth, TJ (1991). "Studies of the uptake of nitrate in barley: III. Compartmentation of NO_3^-." *J. Exp. Bot.* **42**, 1455–1463.
Smith, AM, and Stitt, M (2007). "Coordination of carbon supply and plant growth." *Plant, Cell Environ.* **30**, 1126–1149.
Stephens, DJ, and Allan, VJ (2003). "Light microscopy techniques for live cell imaging." *Science* **300**, 82–86.
Sterky, F, *et al.* (1998). "Gene discovery in the wood-forming tissues of poplar: analysis of 5692 expressed gene sequence tags." *Proc. Natl. Acad. Sci. U.S.A.* **95**, 13330–13335.
Streun, M, *et al.* (2007). "PlanTIS: a positron emission tomograph for imaging ^{11}C transport in plants." *IEEE Nuclear Science Symposium Conference Record* **6**, 4110–4112.
Streun, M, Brandenburg, G, Larue, H, Parl, C, and Ziemons, K (2006). "The data acquisition system of ClearPET Neuro—a small animal PET scanner." *IEEE Trans. Nucl. Sci.* **53**, 700–703.
Swissa, M, Aloni, Y, Weinhouse, H, and Benizman, M (1980). "Intermediary steps in acetobacter-xylinum cellulose synthesis—studies with whole cells and cell-free preparations of the wild-type and a cellulose-less mutant." *J. Bacteriol.* **143**, 1142–1150.
Tanoi, K, Hojo, J, Nishioka, M, Nakanishi, TM, and Suzuki, K (2005). "New technique to trace [^{15}O] water uptake in a living plant with an imaging plate and a BGO detector system." *J. Radioanal. Nucl. Chem.* **263**, 547–552.
Ter-Pergossian, M, Phelps, M, Hoffman, E, and Mullani, N (1975). "A positron-emission transaxial tomograph for nuclear imaging (PETT)." *Radiology* **114**, 89–98.
Thompson, MV (2006). "Phloem: the long and the short of it." *Trends Plant Sci.* **11**, 26–32.
Thornley, JHM (1972). "A balanced quantitative model of root: shoot ratios in vegetative plants." *Ann. Bot. (London)* **36**, 431–444.
Thornley, JHM (1998). "Modeling shoot: root relations: the only way forward?." *Ann. Bot. (London)* **81**, 165–171.
Thorpe, MR, Ferrieri, AP, Herth, MM, and Ferrieri, RA (2007). "^{11}C-imaging: methyl jasmonate moves in both phloem and xylem, promotes transport of jasmonate, and of photoassimilate even after proton transport is decoupled." *Planta* **226**, 541–551.
Thorpe, MR, and Minchin, PEH (1991). "Continuous monitoring of fluxes of photoassimilate in leaves and whole plants." *J. Exp. Bot.* **42**, 461–468.
Thorpe, M, Walsh, K, and Minchin, P (1998). "Photoassimilate partitioning in nodulated soybean: I. ^{11}C methodology." *J. Exp. Bot.* **49**, 1805–1815.
Turgeon, R (1987). "Phloem unloading in tobacco sink leaves: insensitivity to anoxia indicates a symplastic pathway." *Planta* **171**, 73–81.
Turgeon, R, and Wimmers, LE (1988). "Different patterns of vein loading of exogenous [^{14}C] sucrose in leaves of *Pisum sativum* and *Coleus blumei*." *Plant Physiol.* **87**, 179–182.
Tyson, JJ, Chen, KC, and Novak, B (2001). "Network dynamics and cell physiology." *Nat. Rev. Mol. Cell Biol.* **2**, 908–916.
Tyson, JJ, Chen, KC, and Novak, B (2003). "Sniffers, buzzers, toggles and blinkers: dynamics of regulatory and signaling pathways in the cell." *Curr. Opin. Cell Biol.* **15**, 221–231.
Uchida, H, Okamoto, T, Ohmura, T, Shimizu, K, Satoh, N, Koike, T, and Yamashita, T (2004). "A compact planar positron imaging system." *Nucl. Instrum. Methods Phys. Res. A* **516**, 564–574.
Van As, H (2007). "Intact plant MRI for the study of cell water relations, membrane permeability, cell-to-cell and long distance water transport." *J. Exp. Bot.* **58**, 743–756.
Wang, MY, Siddiqi, MY, Ruth, TJ, and Glass, ADM (1993a). "Ammonium uptake by rice roots: I. Fluxes and subcellular distribution of $^{13}NH_4^+$." *Plant Physiol.* **103**, 1249–1258.
Wang, MY, Siddiqi, MY, Ruth, TJ, and Glass, ADM (1993b). "Ammonium uptake by rice roots: II. Kinetics of $^{13}NH_4^+$ influx across the plasmalemma." *Plant Physiol.* **103**, 1259–1267.
Weijer, C (2003). "Visualizing signals moving in cells." *Science* **300**, 96–100.
Williams, J, Minchin, P, and Farrar, J (1991). "Carbon partitioning in split root systems of barley: the effect of Osmotica." *J. Exp. Bot.* **42**, 453–460.
Windt, CW, Vergeldt, FJ, De Jager, PA, and Van As, H (2006). "MRI of long-distance water transport: a comparison of the phloem and xylem flow characteristics and dynamics in poplar, castor bean, tomato and tobacco." *Plant, Cell Environ.* **29**, 1715–1729.
Zhu, XG, de Sturler, E, and Long, SP (2007). "Optimizing the distribution of resources between enzymes of carbon metabolism can dramatically increase photosynthetic rate: a numerical simulation using an evolutionary algorithm." *Plant Physiol.* **145**, 513–526.